Photo-and Electro-Switchable 1/2D Diffractive Structures Exploiting Soft-Matter

Luciano De Sio

University of Calabria
Department of Physics
87036 Arcavacata di
Rende, 87036
Italy

Report Date: May 2013

Final Report from 14 November 2011 to 13 November 2012

Air Force Research Laboratory
Air Force Office of Scientific Research
European Office of Aerospace Research and Development
Unit 4515 Box 14, APO AE 09421

REPORT DOCUMENTATION PAGE

Form Approved OMB No. 0704-0188

Public reporting burden for this collection of information is estimated to average 1 hour per response, including the time for reviewing instructions, searching existing data sources, gathering and maintaining the data needed, and completing and reviewing the collection of information. Send comments regarding this burden estimate or any other aspect of this collection of information, including suggestions for reducing the burden, to Department of Defense, Washington Headquarters Services, Directorate for Information Operations and Reports (0704-0188), 1215 Jefferson Davis Highway, Suite 1204, Arlington, VA 22202-4302. Respondents should be aware that notwithstanding any other provision of law, no person shall be subject to any penalty for failing to comply with a collection of information if it does not display a currently valid OMB control number.
PLEASE DO NOT RETURN YOUR FORM TO THE ABOVE ADDRESS.

1. REPORT DATE *(DD-MM-YYYY)*	2. REPORT TYPE	3. DATES COVERED *(From – To)*
21 May 2013	**Final Report**	**14 November 2011 – 13 November 2012**

4. TITLE AND SUBTITLE

Photo-and Electro-Switchable 1/2D Diffractive Structures Exploiting Soft-Matter

5a. CONTRACT NUMBER

FA8655-12-1-0003

5b. GRANT NUMBER

Grant 12-0003

5c. PROGRAM ELEMENT NUMBER

61102F

6. AUTHOR(S)

Luciano De Sio

5d. PROJECT NUMBER

5d. TASK NUMBER

5e. WORK UNIT NUMBER

7. PERFORMING ORGANIZATION NAME(S) AND ADDRESS(ES)
University of Calabria
Department of Physics
87036 Arcavacata di
Rende, 87036 Italy

8. PERFORMING ORGANIZATION REPORT NUMBER

N/A

9. SPONSORING/MONITORING AGENCY NAME(S) AND ADDRESS(ES)

EOARD
Unit 4515
APO AE 09421

10. SPONSOR/MONITOR'S ACRONYM(S)

AFRL/AFOSR/IOE (EOARD)

11. SPONSOR/MONITOR'S REPORT NUMBER(S)

AFRL-AFOSR-UK-TR-2013-0022

12. DISTRIBUTION/AVAILABILITY STATEMENT

Distribution A: Approved for public release; distribution is unlimited.

13. SUPPLEMENTARY NOTES

This was originally started as Grant 11-3042 but not awarded until FY12 as Grant 12-0003.

14. ABSTRACT

Photosensitive Liquid Crystals (PLC's) are promising materials in the photonics field as they combine the photosensitivity of photochromic molecules such as azobenzene-based materials with the high birefringence that is typical of liquid crystals. By exposing azobenzene molecules to suitable wavelength radiation, they undergo a conformational change (trans-cis isomerization) which can occur in nanoseconds and which can drive the liquid crystal through an isothermal nematic-isotropic phase transition. This photo-induced isotropic state possesses a much different refractive index and the ability to switch between these two states enables e ultra-fast photonic devices of tremendous scientific and technological interest. In addition, the possibility to confine and stabilize PLC's has been very recently examined by our group. Confinement in an anisotropic structure with periodicity on the order of the radiation wavelength leads to the creation of novel diffractive structures (termed H-PDLCs) whose optical properties can be switched using an electric field. The possibility to realize an optically controllable photonic device by combining the photosensitivity of azobenzene materials and the optical properties of H-PDLCs is of tremendous interest to Air Force applications. This was accomplished during this grant, and multiple characteristics and properties of H-PDLCs measured and confirmed.

15. SUBJECT TERMS

EOARD, Photosensitive Liquid Crystals, PLC's, isothermal nematic liquid crystals, H-PDLCs

16. SECURITY CLASSIFICATION OF:			17. LIMITATION OF ABSTRACT	18, NUMBER OF PAGES	19a. NAME OF RESPONSIBLE PERSON
a. REPORT UNCLAS	**b. ABSTRACT** UNCLAS	**c. THIS PAGE** UNCLAS	SAR	21	John Gonglewski

19a. NAME OF RESPONSIBLE PERSON
John Gonglewski

19b. TELEPHONE NUMBER *(Include area code)*
+44 (0)1895 616007

Standard Form 298 (Rev. 8/98)
Prescribed by ANSI Std. Z39-18

Air Force Office of Scientific Research
Air Force Materiel Command, USAF

Basic Research entitled: "Photo-and Electro-Switchable 1/2D Diffractive Structures Exploiting Soft-Matter"

Grant number FA8655-12-1-0003

Principal Investigator: **Luciano De Sio**

Department of Physics University of Calabria

87036 Arcavacata di Rende, Italy

FINAL REPORT

Rende, May 14th, 2013

1. Project organization, management, expenses

a) <u>Travels</u>

The principal investigator of the project was visiting the Beam.Co (Orlando-Florida) for four months (August-September 2012), (April-May 2013).

b) 1 year of Ph.D scholarship has been supported

c) <u>Expendable supplies and materials</u>

Some consumables and optical elements have been purchased, which were necessary for the fabrication of samples

d) <u>People working and collaborating at the project</u>

Giovanna Palermo, Vincenzo Caligiuri, Cesare Umeton (University of Calabria)

Svetlana Serak, Nelson Tabiryan (Beam.Co)

Timothy Bunning (Air Force Research Laboratory)

Scientific Report

Task 1: *Realization of electro-switchable and all-optical POLICRYPS structures by using both single step and multi-step fabrication processes.*

We started our research activity by exploiting in details the optical and electro-optical properties of a soft composite diffraction grating called POLICRYPS (acronym of alternation of POLymer - LIquid CRYstal - Polymer Slices). This is made of slices of almost pure polymer, alternated to films of well aligned Nematic Liquid Crystals (NLC). The structure is obtained by irradiating with an interference pattern of UV light, and under suitable experimental and geometrical conditions, a homogeneous syrup of NLC (E7, by Merck) and pre-polymer NOA-61 (by Norland) containing a UV sensitive photoinitiator. The curing process is carried out at a 100 nm precision level, by utilizing an optical holographic setup, which enables the spatial periodicity of the structure to be easily varied from the almost nanometric to the micrometric range.
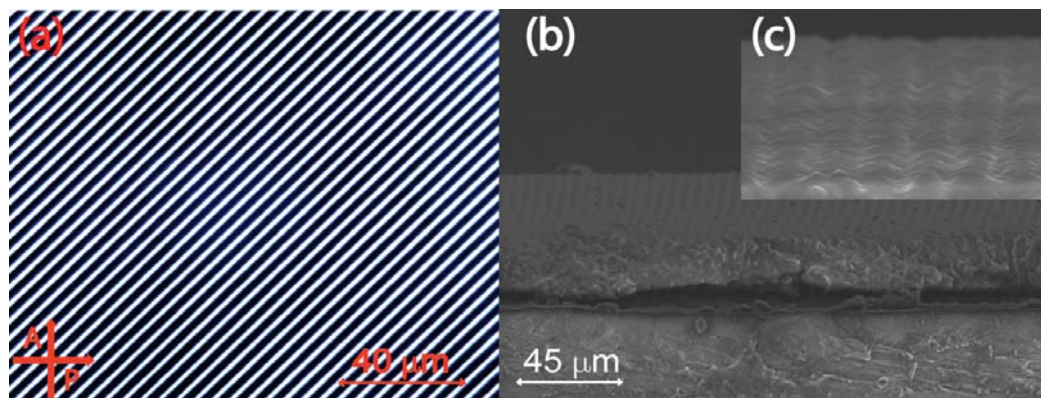
Fig. 1: Polarized Optical Microscope (POM) micrograph (**a**), and ESEM side view (**b**), along with its high magnification (**c**), of a typical POLICRYPS structure.

The POM view of a POLICRYPS structure with a periodicity of $\Lambda= 5$ μm, reported in Fig. 1**a**, reflects the almost complete phase separation that is usually achieved in this kind of systems and evidences the absence of LC droplets, whose presence could yield some scattering of the impinging light and some depolarization of the transmitted/diffracted one. Fig 1**b** is a side view of the POLICRYPS structure acquired by means of an Environmental Scanning Electron Microscope

(ESEM) after removing the top cover glass. The sample response has been investigated by means of an optical spectrometer, which enabled detection of polarized diffraction spectra.
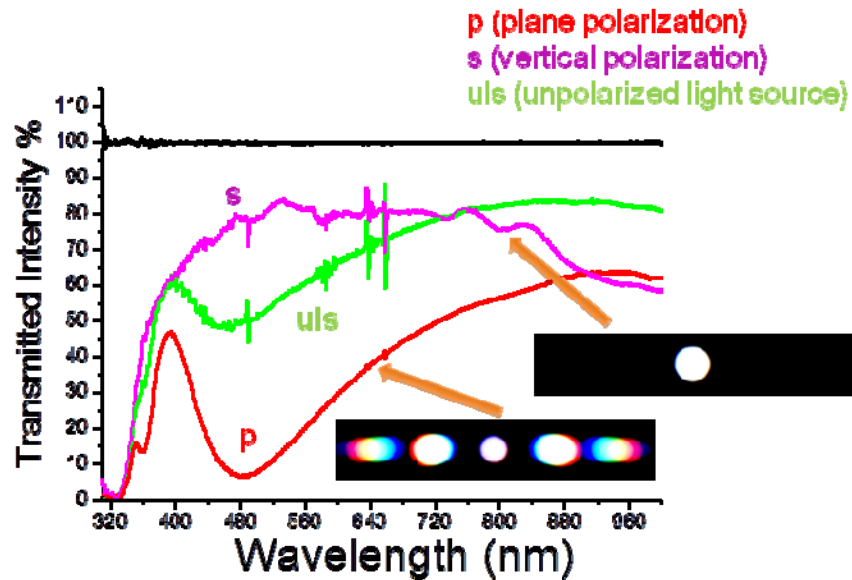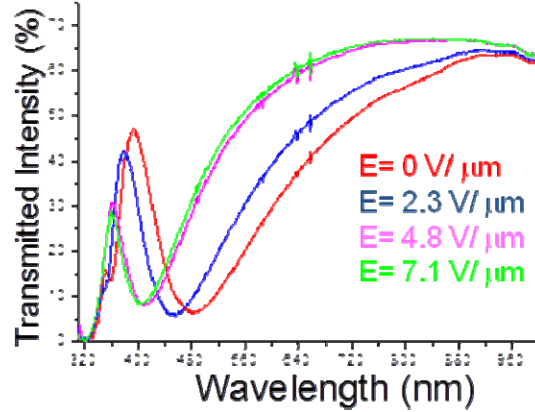

Fig. 2: Spectral response of the sample for two impinging orthogonal polarizations (magenta and red curve) and for an unpolarized light source (green curve)

Fig. 2 shows the transmission of the sample for two impinging, orthogonal, polarizations; **p**-polarized light experiences a large refractive index modulation, since $n_p \neq n_e$ (n_p and n_e indicate the polymer and the NLC extraordinary refractive index, respectively). Therefore, the transmitted wave exhibits a band-gap due to the strong diffraction operated by the structure in this spectral range (red curve), as shown by the far field diffraction pattern,. On the contrary, **s**-polarized light experiences a low index modulation (since $n_p \sim n_o$, where n_o is the NLC ordinary refractive index) and the transmitted light exhibits a spectrum (magenta curve) whose shape is similar to the impinging light one (back curve). In order to check the influence of the grating refractive index contrast on the position of the band-gap, we have investigated the spectral response of the sample by probing it with linearly polarized (p-polarization) white light, at normal incidence, while increasing the amplitude of the applied electric field; results are reported in Fig. 3.

Fig. 3: Spectral response of the of the sample for different values of the applied electric field amplitude.

By increasing the amplitude of the applied electric field, due do the induced NLC director reorientation, the impinging probe radiation experiences, in the NLC films of the POLICRYPS structure, a refractive index which gradually varies from n_e to a values that results very close to n_o. In this way, the grating refractive index contrast Δn_g (defined as the difference between the refractive index of the polymer and the NLC one) undergoes a variation that induces a blue shift of the diffraction band of about 100 nm (Fig. 3). This behavior can be explained in the framework of the Kogelnik theory; in fact, the diffraction efficiency of a periodic structure can be described by means of the following equation:

$$\eta = \sin^2\left[\frac{\pi \cdot \Delta n_g \cdot L}{n_0 \cdot \lambda \cdot \cos\beta}\right] = \sin^2\left[\varphi(L, \lambda, \Delta n_g(E,T))\right] \tag{1}$$
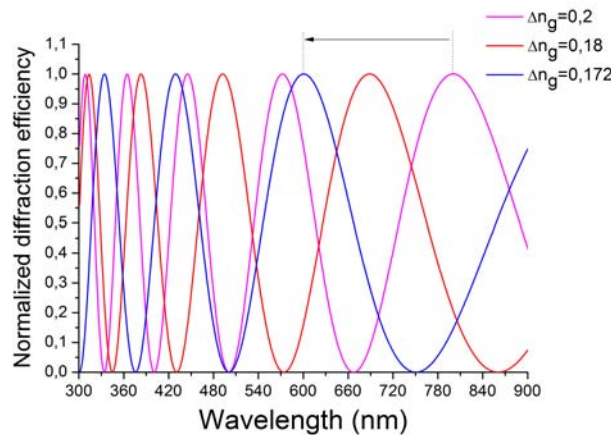
Fig. 4: Plot of the diffraction efficiency versus the impinging probe wavelength while varying Δn_g

Where the argument ϕ depends mainly on grating thickness L, probe wavelength λ and Δn_g. It is easy to observe from the plots of eq. 1 reported in Fig. 4 that by decreasing gradually Δn_g we can keep η constant for small values of λ (blue shift range).
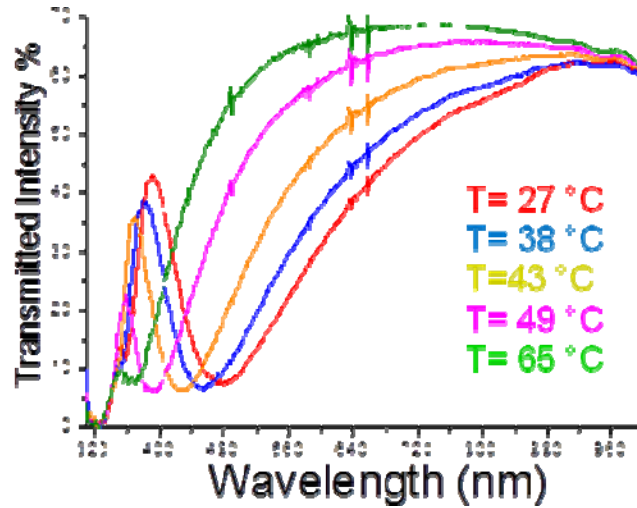

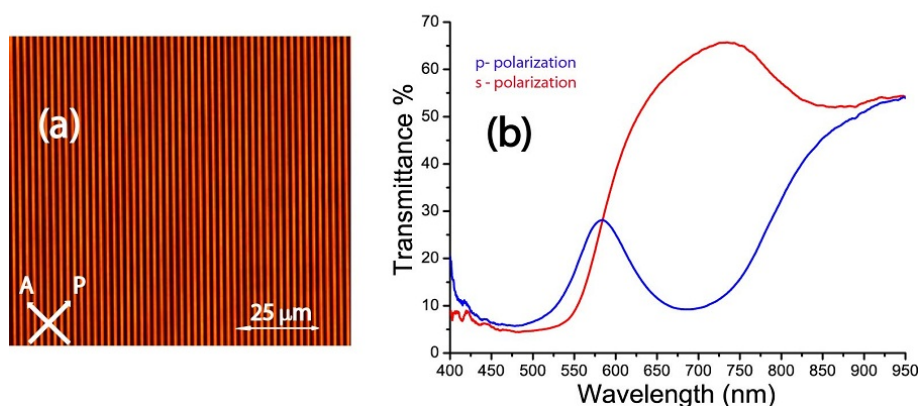**Fig. 5**: Spectral response of the sample versus its temperature.

An additional demonstration of the tunability of the diffraction of our composite structure has been obtained by varying its temperature; results are reported in Fig. 5. By means of a miniature oven, it was possible to vary the sample temperature from 27 °C up to 65 °C; due to the Nematic to Isotropic transition of the NLC component, Δn_g was gradually reduced, with a consequent blue shift ($\approx$ 150 nm) of the diffraction band.

A further important goal of this project is in the possibility of controlling light by exploiting light instead of electric signals. The development of Photoresponsive Liquid Crystals (PLCs) has provided compelling solutions for all-optical switching applications. PLCs are Liquid Crystals (LCs) containing an azo-group in their structure, thus exhibiting both the photosensitivity of azobenzene compounds and the high birefringence of LCs.

The POLICRYPS, which has been initially designed and exploited as a high quality, switchable, diffraction grating, represents also an excellent candidate for realizing an empty periodic polymeric template. Indeed, we have recently shown that, starting from a POLICRYPS

grating, it is possible to remove the LC from the polymeric structure by dipping the sample in a water solution of tetrahydrofuran (THF); in this way, a capillary flow washes out the LC from the micro-channels in a "selective way"(microfluidic etching), without affecting the morphology of the polymeric structure. Then, we have infiltrated the empty POLICRYPS template with a new generation of PLC named "CPND-57", which is a mixture of the piperazine-based push-pull LC azo dyes CPND 5 and CPND 7 (BEAM Engineering). During the whole filling process, the sample was kept at a fixed high temperature (70 °C), which ensured a complete transition to the isotropic state of the LCs (T_{N-I} = 67 °C). After the filling process came to an end, by slowly (0.5 deg/min) cooling down the sample to room temperature, a self-organization process was induced, which gave rise to a uniform and permanent alignment of the PLC within the micro-channels; the excellent optical quality of the sample is evident in the POM view of Figure 6a.

Fig. 6: POM micrograph (**a**) and spectral response of the sample for two orthogonal impinging polarizations (**b**)

We have checked the PLC alignment inside the polymeric template by performing a polarized transmission spectrum. Fig. 6b shows the transmission of the sample for two impinging, orthogonal, polarizations: due to the good alignment of the director, **p**-polarized light experiences a large index modulation (since $n_p \neq n_e$) and therefore the transmitted light exhibits a band-gap, which is due to the strong diffraction of the structure in this spectral range (blue curve). On the contrary, **s**-polarized light experiences a low index modulation (since $n_p \sim n_o$) and the impinging light is totally transmitted (red curve).
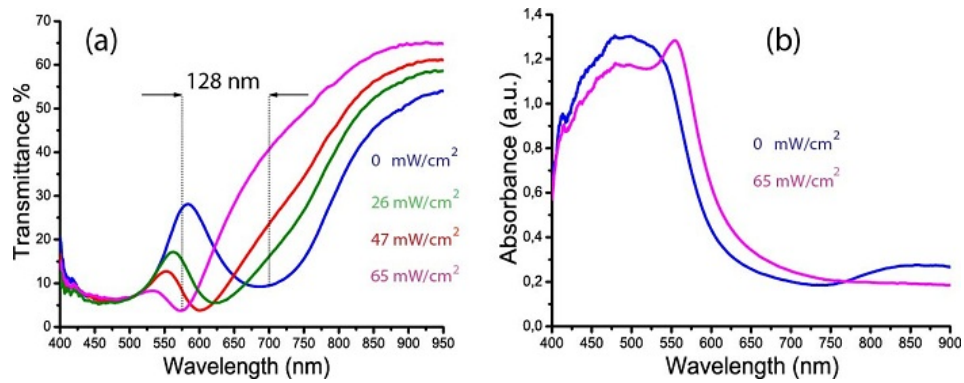
Fig. 7: Spectral response versus the external pump power for **p**-polarized light (**a**) and **s**-polarized light (**b**)

We have analyzed the dynamics of the transmission spectra (Fig. 6b) by means a standard pump-probe setup; we acquired the transmission spectrum (p-polarized light source) while irradiating the sample with a CW laser beam (λ_{pump}= 488 nm). The pump beam induces a photo-chemical phase transition (trans to cis photoisomerization) of the PLC which destroys the LC order; the illuminated area becomes, therefore, locally isotropic. In fact, by increasing the pump power density (Fig. 7a) the NLC order is gradually destroyed (consequently Δn_g is reduced) and the grating diffraction band is blue shifted of about 128nm. Also in this case, the observed behaviour is in agreement with the Kogelnik model, previously described. In addition, we have repeated the experiments by monitoring the absorption spectrum (s-polarized light source) while illuminating the sample with the same pump beam. We observed (Fig. 6b) a partial reduction of the principal absorption (450-550 nm) and a new absorption peak (Fig. 6b, magenta curve) around 580 nm, which is due to the occurred *trans to cis* photochemical transition.

Finally, we have investigated the most interesting aspect related to this first task of the project: by means of a pulsed pump beam, we have analyzed the response time of our light sensitive structure. In fact, we have realized a test setup consisting of a pump and probe beam subsets. The probe beam subset uses a diode laser (λ = 635 nm) while the pump is a nanosecond laser provided by the second harmonic generation of a Nd:YAG laser (λ=532 nm).
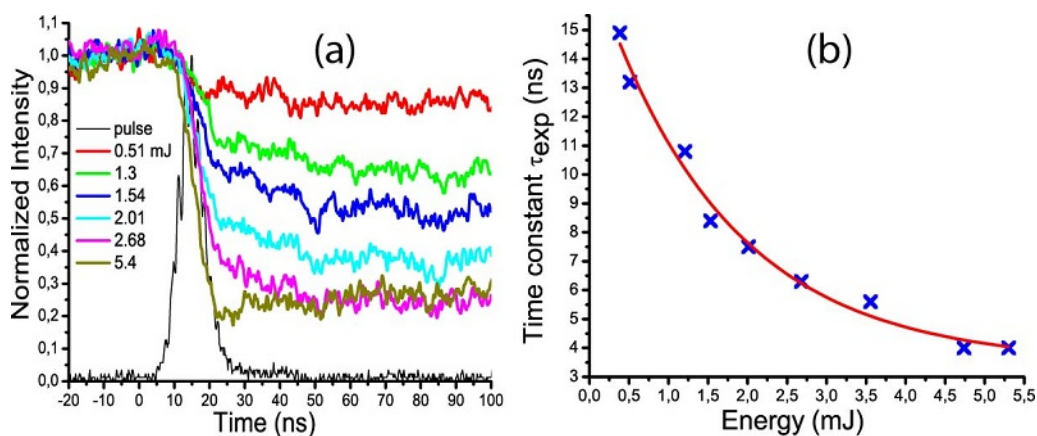
Fig. 8: Diffracted intensity (a) and response time (b) versus the pump energy

We have investigated the dynamics of the sample by varying the pump energy (from 0.51 mJ to 5.4 mJ) while the probe power was kept constant. Fig. 8a demonstrates the effect of a single laser pulse (beam diameter 1.2 mm) on the transmission (first-order diffraction) of the probe laser. By increasing the energy of the pump beam, the diffracted intensity is gradually reduced due to the induced ultra-fast trans to cis photoisomerization process. The switching times of each curve are plotted in Fig. 8b versus the impinging pump energy (data are well fitted by a negative exponential curve). This behaviour can be explained by assuming that the rate of concentration of the photoisomerized PLC molecules is proportional to the impinging pump energy. It is worth nothing that the energy of the pulse is not sufficient to totally switch off the diffracted beam if we want to avoid damaging the sample; however, it is very important to remark that, by exploiting the outstanding properties of PLC materials, we can get nanoseconds response time for liquid crystalline compounds.

Task 2: *Active Plasmonic nanomaterials*

We have synthesized Cetyltrimethylammonium bromide (CTAB) capped, water based, Gold Nanorods (GNRs) and subsequently transferred them in chloroform, since Liquid Crystals(LCs) do not dissolve in water. Transmission Electron Microscopy (TEM, by Jeol JEM-1011 microscope, operating at 100 kV) analyses have been performed by depositing one droplet of different aqueous GNR dispersion onto a carbon-coated copper grid, and then allowing the aqueous solvent to evaporate. For a statistical determination of the average GNR size, shape and aspect ratio, at least 200 objects have been counted for each investigated sample.
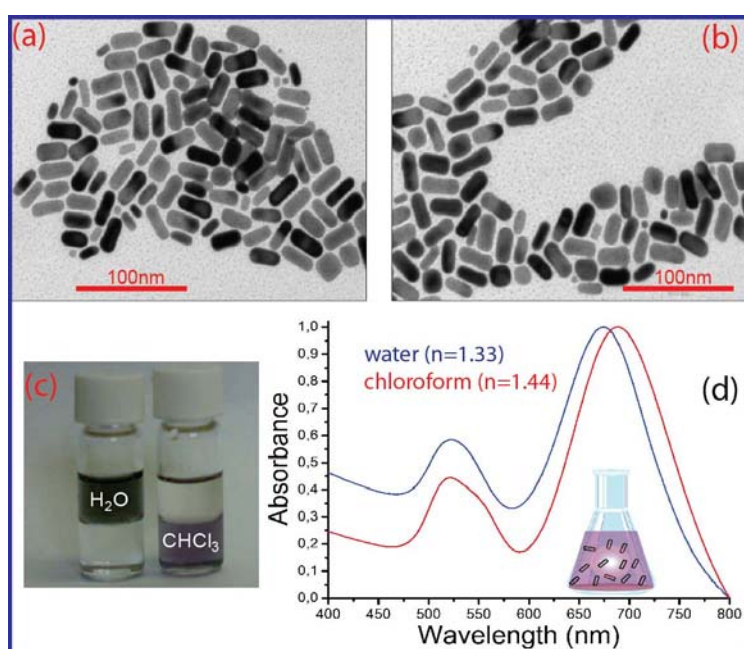
Figure 1. TEM images of water-solution (a) and chloroform-solution (b) of GNRs. Picture of vials with GNR solution in water and in chloroform after phase tranfer process (c). Normalized UV-Vis absorption spectra (d) for water (blue line) and chloroform (red line) solutions of GNRs.

The TEM image of Figure 1**a** confirms that the particle population consists mainly of GNRs with a 2.5 ± 0.4 Aspect Ratio (AR). All the GNRs were successfully extracted into the chloroform by exploiting decanoic acid. This molecule electrostatically binds to the CTAB bilayer on the one side (which confers a positive charge to the GNR surface) by means of a deprotonated carboxylic group, while, from the other side, it shows the alkylic group, towards the chloroform to assure the solubility in organic solvent. The TEM image of GNRs cast from chloroform, shown in Figure 1**b**

confirms that no change in shape and size of particles occurred upon the transfer in organic solvent. In Figure 1**c**, the picture shows the occurred transfer of GNRs from water, in the upper part of the bifasic solution, to chloroform, where the presence of GNRs in the solution is well evident (lower and blue coloured part). Normalized UV-Vis absorption spectra of GNRs before and after the water to chloroform are shown in Figure 1**d**. The water based GNR solution exhibits two typical plasmon bands: a transverse one at 520 nm and a longitudinal one at 674 nm (Figure 1**d**, blue line). The spectral features are retained after the transfer of GNRs into chloroform, although the peak wavelength of the longitudinal band is red-shifted. This effect can be explained by taking into account that optical properties of ellipsoidal particles can be predicted in the framework of the Gans theory[22], through the expression of the extinction cross section:

$$\sigma_{abs} = \frac{2\pi V}{3\lambda} \varepsilon_m^{3/2} \sum_{j=a,b,c} \frac{(1/P_j^2)\varepsilon_2}{(\varepsilon_1 + (1-P_j)\varepsilon_m / P_j)^2 + \varepsilon_2^2} \tag{1}$$

where V is the volume of the particle, λ is the wavelength of light, ε_m is the dielectric constant of the surrounding medium, ε_1 and ε_2 are the real and imaginary parts of gold dielectric constant, respectively, while the depolarization factors P_j are defined by:

$$P_a = (\frac{1-e^2}{e^2})\left\{\frac{1}{2e}\ln\left(\frac{1+e}{1-e}\right) - 1\right\}; \ P_b = P_c = \frac{1-P_a}{2} \tag{2}$$

where a, b, and c stand for the dimensions of GNRs along their three axes. Typically, a > b = c, e = (1- (1/AR)^2)$^{1/2}$, and AR is the aspect ratio of the GNRs. Based on this theory, for small and isolated GNRs, the spectral position of the Localized Plasmon Resonance (LPR) peaks depend on the refractive index of the surrounding medium, according to the condition that minimizes the denominator of equation 1:

$$\varepsilon_1 = -((1-P_j)\varepsilon_m / P_j) \tag{3}$$

According to this equation, a modification in the dielectric behavior of the host material can take place along each coordinate axis. In fact, if ε_m increases, the resonance condition is fulfilled for higher absolute values of ε_1. Now, it is well known that, in the visible range, the absolute value of the real part of the electric permittivity of Gold NPs increases with λ; therefore, fulfillment of

equation 3 takes place for higher values of λ. In our case, due to the variation of the refractive index of the surrounding medium (from 1.33 to 1.44) the longitudinal plasmon band of the chloroform GNRs solution (Figure 1**d**, red curve) is red-shifted of about 15 nm with respect to the water-solution of GNRs (Figure 1**d**, blue line). It is worth noting that the transverse band (520 nm) does not exhibit any shift due to the low sensitivity to refractive index variation; Incidentally, this behaviour indicates a high sensitivity of the longitudinal plasmon band to variation of the refractive index of the surrounding medium.

In order to obtain a homogeneous mixture, the GNRs have been mixed into the CLC at different concentration, up to 10% in weight. The CLC has been prepared by twisting a Nematic LC (MDA-00-1444, by Licristal) with a 20% in weight of chiral agent (ZLI-811, by Licristal) obtaining a helix pitch of about 400 nm. First of all, we observed that GNRs red-shifted the typical reflection band of the CLC. Thus, in our experiments, we have used the mixture with the highest concentration of GNRs (10 wt.% , the CLC reflection band is pushed to NIR) and then we have added the chiral agent (7% wt) for pulling back the reflection band to the visible range (peak of the reflection band ≈526nm). We have then filled (at room temperature, by capillarity) a 100μm thick glass cell treated with a thin polyimide layer, where existence of a preferred planar direction has been induced via rubbing.
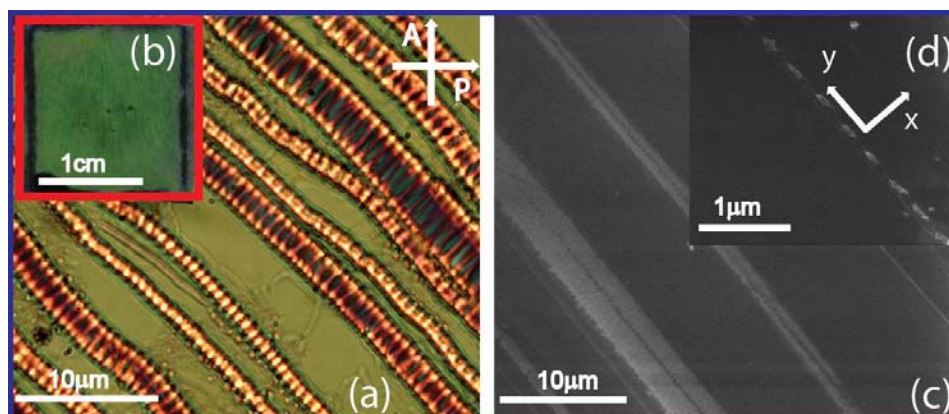
Figure 2. POM view (**a**) of the sample (**b**) along with the SEM image of morphology (**c**) and its high magnification (**d**)

Figure 2**a** is a Polarized Optical Microscope (POM) view of the sample, where the presence

of structural defects, called oily streaks is evident. In a flat cell, with layers parallel to the bounding plate, oily streaks appear as long bands that separate ideal domains of the flat layers. The inner structure of these domains is quite complicated and depends on many parameters, such as elastic constants, surface anchoring, cell thickness and GNRs concentration. In any case, oily streaks are markers of a lamellar phase and clearly confirm the existence of a Grandjean texture (that means CLC helix axis oriented perpendicularly to the glass surfaces) of the CLC phase. In order to study the effects produced by the presence of GNRs, we first tried to figure out their distribution within the CLC by performing an Electron Back-Scattering Diffraction (EBSD) characterization of the sample. This analysis is valuable to distinguish gold from other materials in sample since the yield of backscattered electrons is proportional to specimen atomic number (Z); in our case, the gold (Z=79) produces a high contrast with the CLC surrounding (a carbon based system with Z~15). As shown in the EBSD view of Figure 2**c**, the bright stripes indicate a presence of gold in the oily streaks only, while in the high magnification (Figure 2**d**), we can notice that GNRs are very well oriented along the y direction. It is also worth noting that, despite the circumstance that AR remains almost unchanged, the average size (length and diameter) is increased of about 2-3 times due to an effect of aggregation of GNRs.

It is well known that, on a CLC system in a planar configuration (helical axis perpendicular to the plane of the cell) , a circularly polarized light of the same handedness as the helix and having wavelength between n_oP and n_eP (n_o and n_e being the ordinary and extraordinary refractive indices of the material, respectively and P being the pitch) is reflected by the CLC layer at normal incidence. Light of the opposite handedness propagates, unaffected, through the CLC. For unpolarized light in the wavelength range $n_oP < \lambda < n_eP$, an ideal sample reflects therefore 50% of the impinging intensity and transmits the remaining 50%, whereas the sample remains transparent to light outside that range. The center of the reflection band occurs at:

$$\lambda_0 = \langle n \rangle \, P \tag{4}$$

where $\langle n \rangle = (n_e + n_o)/2$ is the average refractive index, while the bandwidth is given by:

$$\Delta\lambda = \Delta n\, P = (n_e - n_o)P \tag{5}$$

The CLC pitch P is sensitive to all the factors (e.g. temperature) that can affect the balance of molecular interactions and the orientation of the CLC director. Therefore, we have performed experiments devoted to understanding the influence on the CLC configuration of the local heating induced by a suitable optical radiation trough the GNR resonance. To this end, we have realized the all-optical setup reported in Figure 3.
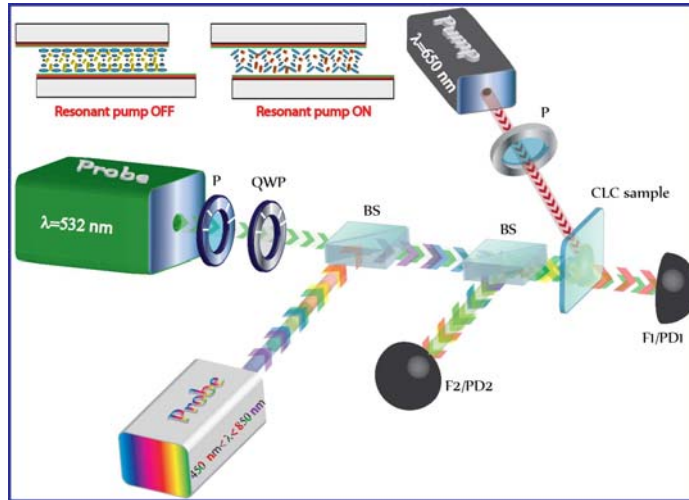
Figure 3.All-optical setup for sample characterization. P: polarizer; QWP: quarter waveplate; BS: beam splitter; $F_{1,2}$: transmission and reflection fibers; $PD_{1,2}$: photodetectors. In the top-left it is reported a sketch of the sample configuration with and without the influence of the pump beam.

This setup utilizes a low power density (P_{probe}=0.1W/cm^2) CW probe laser, emitting at λ=532nm, in the center of the reflection band ($\lambda_0 \approx$526nm), a collimated and co-launched white source (450nm< λ<850 nm) for monitoring the spectral reflection properties of the CLC configuration, and a CW NIR pump laser emitting at λ=650 nm (P_{pump}= 0.3 W/cm^2) in the high absorption range (longitudinal band) of the GNRs. In a first attempt, we have probed the sample by using the white light source and monitoring its back reflected components by means of the reflection fiber (F2).

1. Plasmonic control of photonics bandgap

Figure 4**a** reports the behavior of the reflection band under illumination with the pump beam for different exposure times. The CLC configuration (inset Figure 3, resonant pump off) acts as a

mirror for all the wavelengths within the reflection band of the impinging white light, which are back reflected. Then, by optically pumping the same sample area, the photoexcitation of GNRs induces the formation of heated electron gas that subsequently cools rapidly (*ps* process) by exchanging energy with the GNR lattice; this process is followed by phonon-photon interaction where the GNR lattice cools rapidly by exchanging energy with the surrounding medium
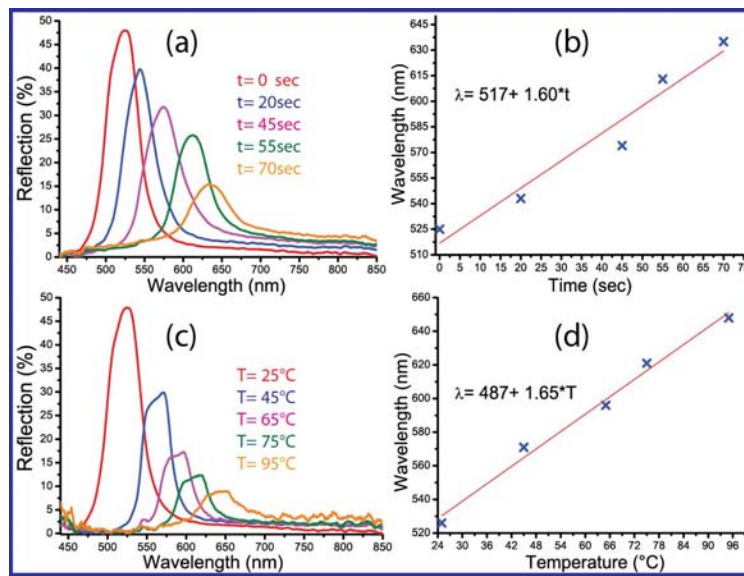
Figure 4. Reflection spectra of the sample for different values of illumination time (**a**) and temperature (**c**); linear fit of the position of the center of the reflection band versus the illumination time (**b**) and temperature (**d**)

The local-heating induces a variation of the CLC pitch (inset Figure 3, resonant pump on) with a consequent linear red-shift of the reflection band. In Figure 4**a**, it is easy to observe that, by keeping constant the pump power and increasing the exposure time, the local temperature is gradually enhanced, with a consequent linear red shift (more than 130 nm, Figure 4**b**) and partial suppression of the reflection band. Indeed, according to equation 4, the center wavelength of the reflection band is directly proportional to the pitch *P* which increases with temperature; in addition, the elongation of P reduces the number of periods in the bulk of the cell, an effect which explains the attenuation of the reflection band amplitude with temperature. To validate the effect of the GNR-induced local heating on the CLC optical response, we have performed a control experiment by varying the sample temperature from 25°C up to 95°C and monitoring the reflection band behaviour (Figure 4**c**). Once again, a linear red-shift is observed, which clearly confirms that the behavior reported in Figure 4**a** is due to a photo-thermal mechanism; furthermore, it is worth noting

that the two calibration functions reported in Figures 4**b** and 4**d** exhibit, within the experimental error, the same slope. This result shows that, by making use of those two calibration functions, it is possible to measure the temperature around GNRs at a given illumination time.

Time (s)	λ_0 (nm)	Temp. (°C)
0	524	25
20	545	35
45	574	51
55	615	75
70	635	87

Table 1. Correlation between illumination time and temperature around the GNRs obtained by a direct measurement of the position of the reflection band center.

This information is summarized in the calibration Table 1 which indicates in details how it is possible to obtain the temperature value around a GNR. Interestingly, the same experiment can be repeated for any kind of plasmonic NPs (different geometry, different size, etc..) in all those cases in which the measure of the sample temperature under a suitable illumination is a key parameter (e.g. nanomedicine).

2. Photonic control of localized plasmonic resonance

So far, we have discussed and analyzed the possibility to control the photonic properties of a CLC configuration by means of the local heating induced by (resonant) GNRs. The approach proved useful not only for controlling the selective reflection of a CLC but also to build up a method for measuring the temperature in the close environment of the GNRs. One more interesting aspect is represented by possibility to use the local refractive index change of the CLC due to the local heating for controlling the plasmonic response of GNRs.
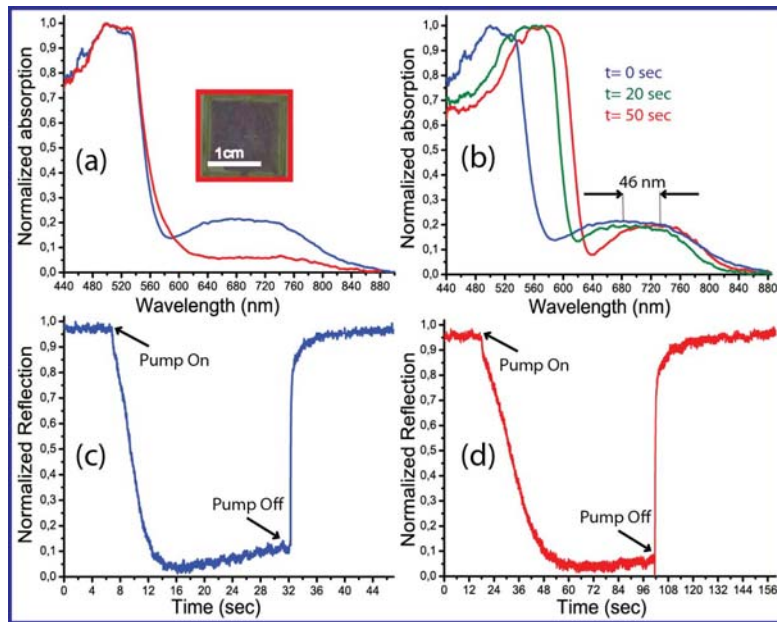
Figure 5. Spectral response of the sample for probe light (white) polarized along x (**a**, red curve) and y (**a**, blue curve). Spectral shift (**b**) of the reflection band and longitudinal LPR by varying the illumination time for probe white light polarized along y. Reflection dynamic response of the sample for pump light polarized along y (**c**) and x (**d**)

Figure 5**a** shows the absorption spectra for two orthogonal impinging polarization of the probe white light. it is worth noting that both polarizations (red and blue curve) exhibit a photonic absorption peak at $\lambda = 520$ nm due to the selective reflection of the CLC configuration, while only the absorption spectrum of the light polarized along the y direction (see Figure 2**d**) exhibit a secondary peak at $\lambda = 680$ nm (blue curve), ascribable to a longitudinal LPR of GNRs. This is a clear indication that GNRs exhibit a preferential organization along the y direction, thus validating the SEM analysis reported in Figure 2**d**. We also stress out that, in these experimental conditions, we did not detect any LPR for a cell thickness less than 100 µm .

In order to check the influence of the local heating on the plasmonic proprieties of the sample, we have observed its spectral response for different values of the pump light illumination time; results are reported in Figure 5**b**. Once again, the local-heating induces a variation of the CLC pitch with a consequent red-shift of the reflection band from 512 nm to 578 nm. Furthermore, due to the CLC refractive index variation, a red-shift of the LPR, from 685 nm to 731nm is observed. This behavior can be explained by considering that the local heating induces gradually a broadened of the oily streaks defects; consequently, the GNRs aggregates can be easily dissolved since

transition from CLC to isotropic phase ensures a better host-fluidity proprieties of the mixture. Indeed, as observed by Kinnan and Chumanov when NPs aggregates are considered, whose size is comparable with the wavelength of the incoming radiation, different areas of the aggregates experience different phases of the incident radiation; thus, higher multipolar modes (quadrupolar, octupolar and even hexadecapolar) have to be taken into account. Given that the excitation frequency of these higher modes is larger than the dipolar one, a macroscopic broadening of the plasmon peak occurs which has its center in the blue region of the electromagnetic spectrum. On the contrary, single, small-sized, NPs, when hit by the incoming radiation, experience the same phase of the electromagnetic wave on their whole area; in this condition, NPs behave as simple dipoles: the plasmonic peak width is quite narrow and, depending on the particle size, the peak is centered in the green–red part of the electromagnetic spectrum. Based on the above considerations, the temperature dependent shift of the plasmonic resonance observed in our sample can be therefore explained in terms of a temperature induced passage from densely packed to mono-dispersed NPs. In fact, for densely packed metal NPs, the absorption peak is quite broad and is centered in the red range (blue curve, Figure 5**b**); due to the increasing of the temperature the GNRs starts to be well separated and the peak slightly reduces its width and shifts to the NIR (red curve, Figure 5**b**).It is worth noting that during this process the value of the refractive index of the CLC is reduced[29,30] and this effect, according to equation 3, induces an opposite blue-shift of the LPR, decreasing the effective red shift. Finally, to check the reversibility and repeatability of the observed effects, we have performed reflection dynamic experiments by using the green probe light of the setup reported in Figure 3 (λ= 532nm, in the middle of the reflection band). By means of PD_2 we have monitored the reflection component when turning On and Off the pump laser; we have observed that, due to the local-heating induced by its light the CLC configuration is gradually destroyed and the reflection component is reduced to zero. On the contrary, when the pump laser is turned off, a CLC self-organization take places and the intensity of the reflection component is restored to its initial value (Figure 5**c**, **d**). It is important to point out that we have observed a strong correlation between the

turn off times and the polarization of the pump laser. Indeed, for light polarized along the *y* direction (Figure 5**c**) the local heating is enhanced (due to the high extinction cross section of the longitudinal LPR), with a corresponding turn-off time of about ≈ 5s, while, light polarized along *x* exhibits a quite slow turn-off time (≈ 30s), due to the low extinction cross section of the transversal LPR. In both cases, we have measured a turn-on time of about 2s. We note that in the spectrum of Figure 5**a** (red curve), the longitudinal LPR is partially overlapped to the reflection band.

f) Publications

- L. De Sio, S. Serak, N. Tabiryan, C. Umeton, T. Bunning "Nanosecond switching of a tunable diffraction band realized in light sensitive diffraction gratings containing liquid crystals", in preparation.

- L. De Sio, V. Caligiuri, N. Tabiryan, C. Umeton, T. Bunning "Electro-optical control of the diffraction light range is soft-composite diffraction gratings" in preparation.

- L. De Sio, Tabiryan, C. Umeton, T. Bunning "Dynamic Photonic Materials based on Liquid Crystals" *Progress in Optics* **2013** (in press)

- M. Romito, L. De Sio**,** A. E. Vasdekis, C. Umeton "Optofluidic microstructures containing liquid crystals Molecular Crystals and Liquid Crystals **2013** (DOI:10.1080/15421406.2013.789716)

- L. De Sio**,** M. Romito, M. Giocondo, A. E. Vasdekis, A. De Luca, C. Umeton *Lab on a Chip*, **2012**, 12, 3760-3765

Luciano De Sio

(Principal investigator)